HEFAT2010
7th International Conference on Heat Transfer, Fluid Mechanics and Thermodynamics
19-20 July 2010
Antalya, Turkey
Paper number:

VORTEX STRUCTURES AND ENTRAINMENT IN CIRCULAR AND DAISY-SHAPED ORIFICE JETS

El Hassan M.*, Meslem A. And Abed-Meraim K.

*Author for correspondence
LEPTIAB,
Université de La Rochelle,
France,
E-mail: elhassanmoh@yahoo.fr

ABSTRACT

The role of streamwise and spanwise vortex structures in the near-field entrainment of a circular and a daisy-shaped orifice jet is investigated experimentally in this paper. Time-resolved stereoscopic PIV measurements are performed in several cross sections perpendicular to the jet axis. Three-dimensional flow field reconstruction based on the stereoscopic PIV results gives better understanding of the three-dimensional features and the different development stages of the jet. The variation of the entrainment rate along the jet axis has been evaluated from the mean velocity field. A higher entrainment is observed in the daisy shaped jet as compared to that of the circular jet. This is due to large-scale streamwise vortical structures generated by the lobed geometry. Strong correlation exists between the entrainment rate and the Kelvin-Helmholtz (K-H) vortices passing for the circular jet. The instantaneous entrainment rate in the daisy jet presents small amplitude variations and is affected by the dynamics of both the azimuthal and the streamwise vortices. The longitudinal development of the mean streamwise vorticity is quite different between the circular and the lobed jets. In the circular jet, the streamwise vorticity becomes more important when traveling downstream along the jet axis and their trajectory is not necessarily linear. The expansion rate of the jet is higher in the minor plane as compared to the major plane in the region of the axis-switching for the daisy jet.

NOMENCLATURE

PIV		Particle Image Velocimetry
POD		Proper Orthogonal Decomposition
K-H		Kelvin-Helmholtz
De	[m]	Equivalent diameter of the jet
U_{0m}	[m/s]	Centreline velocity at the jet exit
U	[m/s]	Streamwise velocity amplitude
u	[m/s]	Streamwise velocity fluctuations
Q_0	[m^3/s]	Initial volumetric flow rate
Q	[m^3/s]	Volumetric flow rate at a given axial position
x	[m]	Cartesian axis direction : longitudinal
y	[m]	Cartesian axis direction : transversal
z	[m]	Cartesian axis direction : vertical
ω_x	s^{-1}	Streamwise vorticity
ω_y *and* ω_z	s^{-1}	Azimuthal components of the vorticity
ω_{yz}	s^{-1}	In-plane vorticity

INTRODUCTION

A quicker and better mixing of the initial region of the jet flow with its ambiance is of considerable interest from practical point of view. The entrainment of ambient air plays an important role in the enhancement of the mixing phenomenon.

Different control strategies have been studied in the literature to enhance the mixing of the jet core with its ambiance. Passive control using non-circular jets was widely proposed to increase the entrainment rate relative to a conventional circular jet. The geometrical modifications of the jet nozzle alter the flow development downstream of the nozzle and seek to enhance the three-dimensionality of the flow, and thus entrainment and mixing, by manipulating the natural development of coherent structures and their breakdown into turbulence [1].

The smooth contraction nozzles [2-7] and the long pipe nozzles [8-11] were the priority of researchers to generate an axisymmetric jet. However, the sharp edged orifice plate [10, 12-15] has received very little attention. Free six-lobed (daisy shaped) and circular orifice jets are investigated in the present study.

In some non-circular jet configurations, the cross-section regularly evolves after a certain distance from the nozzle through shapes similar to those of the jet nozzle but with axes successively rotated at angles characteristic of the jet geometry. In fact, the jet cross-section expands in the direction of the minor axis and contracts in the direction of the major axis, and thereby a 90° switch takes place after a downstream distance [16]. This mechanism, denoted as the axis-switching phenomenon, was observed in elliptic jets [17-21], rectangular jets [22] and lobed jets [23].

The coexistence between the three-dimensional streamwise vortices and the primary two-dimensional vortical structures in jet flows was observed by many authors [24, 25]. The birth and evolution of the streamwise structures depends on both the three-dimensionality of the flow in the jet near-field and the jet exit conditions [25, 26]. Foss [27] suggested that the increase in the pressure hill, formed upstream from a tab placed at the jet exit is believed to be the dominant source of the streamwise vorticity. This mechanism can also explain the streamwise vorticity generation in a lobed orifice jet.

It is known that the azimuthal coherent vortex rings and their merging dominate the shear-layer growth and entrainment in axisymmetric jet configurations [2]. It was also shown in the literature the important role of the streamwise vortices in entraining fluid from the surrounding at longitudinal distances where three-dimensionality becomes the crucial feature of the jet structure [25]. It was noted by Liepmann & Gharib [25] that the streamwise vortex pairs which evolve and amplify in the braid region between primary vortical structures, are shown to drastically alter the entrainment process in the near field and to increase the rate at which the fluid is entrained into the jet. Toyoda and Hiramoto [28] suggested that the entrainment significantly increased by the enhancement of axisymmetric and streamwise vortices. These authors found a low entrainment rate in the braid region and high in the region where streamwise and spanwise vortices interact with each other. The experimental study of McCornick and Bannett [29], on the vortical and turbulent structure in a free shear layer downstream of a lobed mixer, showed that the K-H instability plays a major part in the enhanced mixing process. Mi et al [30] noted that the initial structure of a sharp-edged orifice plate jet is more three-dimensional as compared to the smooth contraction jet.

Although previous studies proved that the large-scale vortical structures play an important role on the entrainment in jet flows, the individual role played by these structures is still unclear and needs to be deeply analyzed. The role played by both the azimuthal and the streamwise vortices is studied in the present work using time-resolved stereoscopic PIV measurements. This technique provides a complete description of the jet flow with high temporal resolution. Thus, the influence of the vortical structures on the entrainment rate for different phases of the vortex passage is obtained. PIV measurements are performed in different longitudinal locations for both the circular and the lobed jets. The global evolution of the circular jet and the axis-switching phenomenon for the daisy lobed jet are explored in the present study.

EXPERIMENTAL PROCEDURE

Air jet facility and orifice jet geometries

Two air jets considered in the present investigation are generated using a circular orifice (figure 1(b)) and a six-lobed daisy orifice (figure 1(c)). These orifices have the same equivalent diameter (De = 16mm) based on the exit area, and are built-up from 1.5mm thick aluminium sheet. The air jet experimental facility consists of an axial miniature fan placed inside a one meter long metallic pipe of 0.16m diameter (figure 1). A convergent duct placed at the end of the pipe ensures the reduction of the turbulence level at the jet exit. A honeycomb structure is positioned just upstream of the convergent duct. The flow rate measured 4 mm downstream from the jet exit is 49×10^{-5} m^3/s for the two jets. The initial Reynolds number based on the centerline exit velocity U_{0m} and on the equivalent diameter De is 3600 for both the jets.

Figure 1 Air jet facility sketch and orifice's geometries

Time resolved PIV measurements

For the vortex dynamics analysis of the studied jets, time-resolved stereoscopic PIV measurements were performed. The instantaneous spatial distribution of the in-plane velocity in the transverse planes at the initial regions of the jets are obtained. The principle of the stereoscopic PIV method was widely discussed in the literature as in articles by Prasad and Adrian [31], Arroyo and Greated [32], Sinha and Kuhlman [33] or the review paper of Prasad [34] among others. The time resolved stereoscopic PIV system used for this study (figure 2) is composed of two Phantom V9 cameras of 1200 x 1632 $pixels^2$ and a Nd : YLF NewWave Pegasus laser of 10mJ energy and 527nm wavelength. The acquisition frequency of the PIV system is 500Hz for a maximal image window. In each plane, a number of 1000 image couples were acquired. The two cameras are mounted on a traversing system with an angle of 45° to the

normal position of the light sheet plane of the laser. The lenses are separated from the camera in order to shift the CCD-chip plane with respect to the lens plane, in a way that the Scheimpflug conditions are satisfied. The stereo reconstruction used in order to obtain the three components of the velocity is an empirical 3D reconstruction [35] based on cross-correlating the two views of the calibration target. The calibrated images give a spatial resolution of 47.1µm per pixel which corresponds to a 77 x 59 mm^2 field of view. Images are processed through an adaptive multi-grid correlation algorithm handling the window distortion and the sub-pixel window displacement. The prediction-correction method is validated for each grid size when the signal to noise ratio of the correlation is above a threshold of 1.1. In average, less than 2% of the vectors are detected as incorrect. These incorrect vectors are corrected by using a bi-linear interpolation scheme. The final grid is composed of 32 x 32 $pixels^2$ size interrogation windows with 50% overlapping leading to a vector spacing of 13.5 pixels which represents a spatial resolution of 0.65 mm. In all the cases, the air jet flows were seeded with small olive oil droplets, 1 to 2 µm in diameter, provided by a liquid seeding generator.

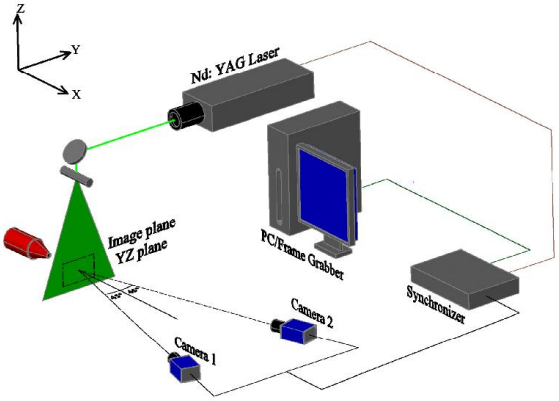

Figure 2 The schematic of the TR stereoscopic PIV system

RESULTS

Role of the azimuthal and streamwise vortices on the entrainment

The entrainment rate in the near field of the circular jet and the daisy-shaped lobed jet is calculated using the following equation:

$$\frac{d(Q/Q_0)}{d(X/De)} = \frac{De}{Q_0}\int_0^{2\pi} r u_r d\theta \qquad (1)$$

Where Q_0 is the initial volumetric flow rate, Q is the volumetric flow rate at the axial distance X from the jet exit plane, De is the jet equivalent diameter, r is the radial distance and u_r is the radial velocity.

A spatial criterion which corresponds to a minimum radial distance of integration is defined for the calculation of the instantaneous entrainment rate. This radial distance corresponds to the convergence of the mean entrainment rate and depends on the axial position [23].

At X/De = 1, it is found that the mean entrainment rate is equal to 0.15 for the circular jet and 0.19 for the lobed jet. On the other hand, the temporal evolution of the entrainment rate shows a higher variation of the entrainment amplitude of the circular jet when compared to the daisy jet (figure 3). The higher mean entrainment rate of the daisy jet as compared to that of the circular jet is related to the presence of large scale streamwise structures in the daisy jet. The dominant feature at the studied longitudinal position (X/De = 1) of the circular jet is the Kelvin-Helmholtz vortex ring. The dynamics of the K-H vortices and their role on the entrainment mechanism could explain the higher variations in the entrainment rate of the circular jet. Therefore, the analysis of the instantaneous velocity fields and the corresponding entrainment rates is necessary to understand the individual role of different vortical structures on the entrainment.

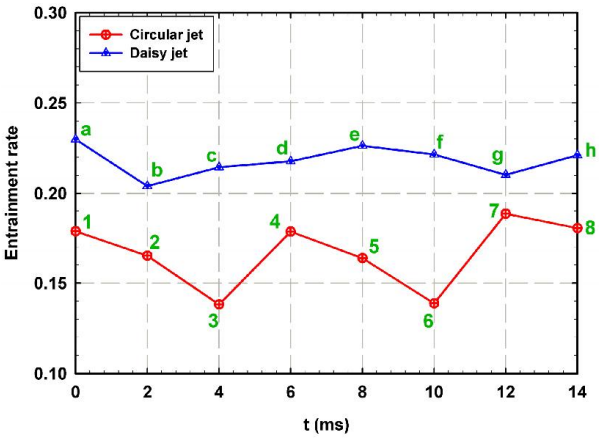

Figure 3 The normalized radial entrainment rate as function of time for the circular jet and the daisy jet at X/De = 1

The vorticity magnitude calculated in the cross-plane (by neglecting the axial derivation of the velocity components) is shown with the three-components of the velocity in the figure 4. For the daisy jet, the instantaneous streamwise vorticity fields illustrate the spatio-temporal evolution of the streamwise vortices (figure 5).

During the K-H ring passing, the velocity distribution near the jet core of the circular jet is highly affected (figure 4). In fact, the front part of the K-H vortex (figure 4 b) expands the flow from the jet center outwards. Similar phenomenon is observed in the downstream part of the K-H vortex ring. In the upstream part of the K-H ring (figure 4 d) and in the braid region (figure 4 a), the flow around the jet core is sucked

inward towards the jet center. This flow dynamics results in variations of the instantaneous entrainment rate. Figure 3 shows an increase of the entrainment rate in the upstream part of the K-H ring and in the braid region. However, the decrease of the entrainment rate is observed for the phases 2 and 3 with a more pronounced decrease being for the phase 3. The time delay between the most expanding zone of the jet flow and the occurrence of the lowest entrainment rate during the K-H passing suggests that the influence of the K-H vortex front part on the ambiance is mainly located just upstream from its location. It should be noted that the streamwise velocity values in the jet core are lower for the phase of the K-H front part as compared to the braid region and the other phases of the K-H vortex passing.

For the daisy jet, the flow dynamics is highly complex at the longitudinal studied position (X/De = 1). At this location, an axis-switching of the flow is present with a strong interaction between the azimuthal and the streamwise vortices. Therefore, the understanding of the role played by these large-scale structures is problematic. In this paper, the analysis of the instantaneous velocity fields and the entrainment rate clearly shows the important role played by the streamwise vortices in the entrainment. In fact, for different phases (figure 5), the streamlines are sucked towards the streamwise structures present around the jet core. Although the variation of the entrainment amplitude is lower in the daisy jet as compared to the circular jet, one should not neglect the phase dependency of the entrainment rate. For example, the phase g on the figure 3 is characterized by a decrease of the entrainment rate. An adverse effect of a K-H vortex could explain the decrease in the entrainment. Such a behavior is confirmed from the snapshot POD (proper orthogonal decomposition) analysis performed by El Hassan and Meslem [23] for the same flow.

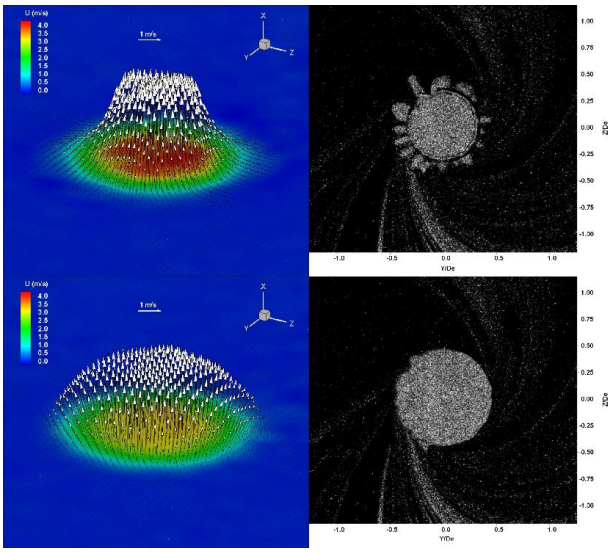

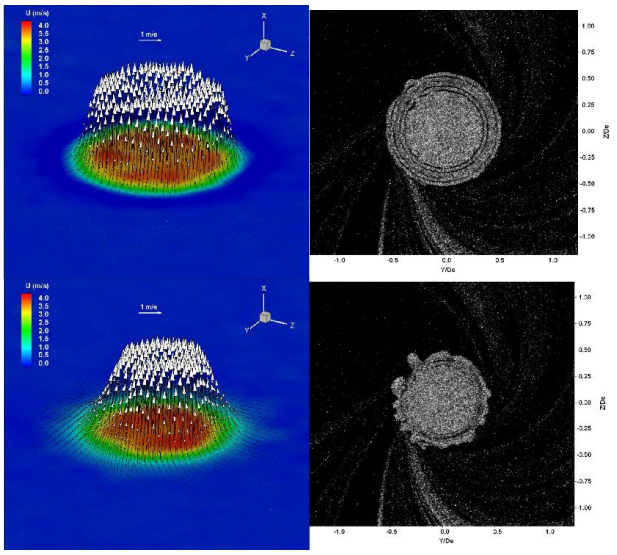

Figure 4 Instantaneous velocity fields and the corresponding flow image in the cross-plane of the circular jet at X/De = 1; respectively phases 1, 2, 3 and 4 of the figure 3

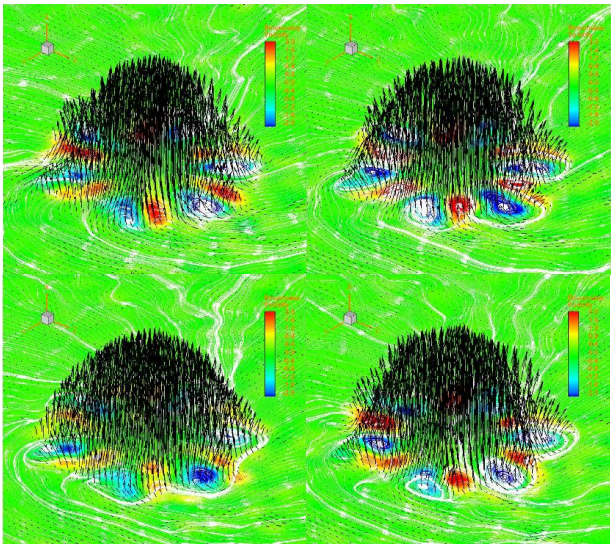

Figure 5 Instantaneous streamwise vorticity and three-components velocity fields in the cross-plane of the daisy jet at X/De = 1; respectively phases e, f, g and h of the figure 3

Three-dimensional reconstruction of the jet flow

The distributions of the three-component ensemble-averaged velocity vectors in the near-field (X/De ≤ 4) of the circular jet are presented in figure 6. The streamwise velocity iso-surfaces and the vorticity magnitude (as colour of the vectors) are also shown on the same figure. It should be noted that the vorticity magnitude is calculated from the in-plane three components of the velocity and thus the out of plane derivation parts were neglected. The representation in the figure 6 is helpful for

showing the downstream evolution of the circular jet. The velocity iso-surfaces illustrate the expansion of the jet and the role of large-scale structures on the evolution of the jet shape. For example, the non-circular shape observed from X/De = 1 results from the development of the streamwise vortices which turns bigger and strengthens when travelling downstream. The vorticity magnitude decreases downstream and is higher around the jet core where the K-H vortex rings develop. Due to interactions of the streamwise vortices between each other, the longitudinal development of these vortices is not necessarily linear [23].

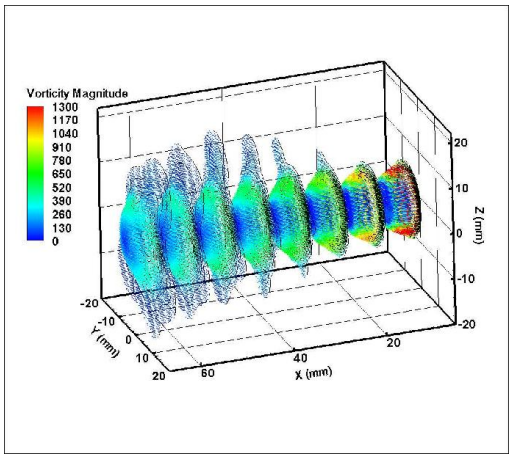

Figure 6 Three-dimensional ensemble-averaged velocity field in the near-field of the circular jet

The flow in the region of the axis-switching is reconstructed from the mean velocity results in 5 cross-planes corresponding to X/De = 0.5, 0.75, 1, 1.5 and 2. Iso-values of the streamwise vorticity and the in-plane vorticity are shown in figure 7. The in-plane vorticity is calculated from the following equation:

$$\omega_{YZ} = \sqrt{(\omega_Y^2 + \omega_Z^2)}$$

Where ω_Y and ω_Z are the azimuthal components of the vorticity.

It is shown from the figure 7 that the streamwise vortical structures emanate from the troughs of the jet orifice and have a linear evolution in the longitudinal direction. The in-plane vorticity mainly represents the azimuthal K-H vortices. Therefore, the shape evolution of the iso-value shown on the figure 7 suggests a deformation of the K-H vortices in the region of the axis-switching. The Biot-Savart deformation of the vortex rings, previously observed for elliptic [19, 20] and rectangular [16] jets, is observed in the present study. In this mechanism, the portions of the vortex with small radius of curvature will move downstream faster than the rest, leading to their deformation. The longitudinal evolution of the momentum thickness, for both the major and the minor planes, in the region of the axis-switching is presented in figure 8. An important expansion rate is observed in the minor plane for 0.5 < X/De < 1 whereas the jet expansion is very low in the major plane. Further downstream, the lobed jet expansion becomes similar in both the minor and the major planes.

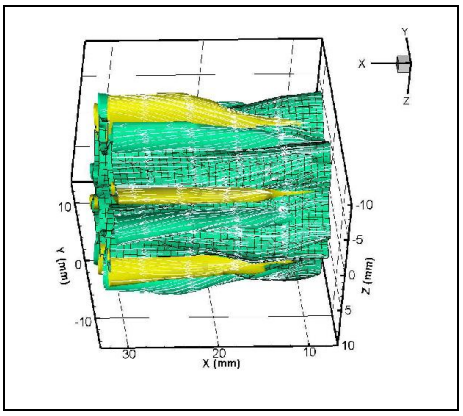

Figure 7 Three-dimensional reconstruction of the lobed jet flow in the region of the axis-switching

Figure 8 Momentum thickness distribution in the major and minor planes in the region of the axis-switching of the daisy jet

CONCLUSION

The entrainment phenomenon and the flow characteristics are investigated in the present paper. The main objective is to study the influence of the large-scale vortical structures on the entrainment at the longitudinal position X/De = 1 for a circular orifice jet and a daisy-shaped lobed orifice jet. This has been achieved using time-resolved stereoscopic PIV measurements. For the circular jet, it is found that the entrainment of the flow from the surrounding towards the jet mainly occurs in the upstream part of the K-H vortex ring and in the braid region. In the downstream part of the K-H vortex, the flow in the circular

jet core and in the K-H location expands outward. At the studied longitudinal position (X/De = 1), the entrainment mainly depends on the dynamics of the K-H vortex ring. The entrainment rate in the daisy jet is higher than in the circular jet, but its amplitude variations are lower in the daisy jet. For the daisy jet, the flow at X/De = 1 is highly complex with strong three-dimensionality and interactions between the azimuthal and the streamwise vortices. The streamwise vortices play a main role in the entrainment of the flow towards the daisy jet core. In addition, the K-H vortex clearly affects the entrainment in the daisy jet. The longitudinal evolution of the streamwise vortices affects the shape of the circular jet in different cross-planes. In the region of the axis-switching, it is seen that the expansion rate is higher in the minor plane as compared to the major plane of the daisy jet.

REFERENCES

[1] Gutmark E.J., and Grinstein E.F., Flow control with noncircular jets. *Annu. Rev. Fluid Mech.,* 1999, vol. 31, pp. 239-272

[2] Crow S.C., and Champagne F.H., Orderly structure in jet turbulence. *J. Fluid Mech.,* 1971, vol. 48, pp. 547-591

[3] Hussein H.J., Capp S.P., and George W.K., Velocity measurements in a high Reynolds number, momentum-conserving axisymmetric turbulent jet. *J. Fluid Mech.,* 1994, vol. 258, pp. 31-60

[4] Hu H., Saga T., Kobayashi T., and Taniguchi N., Research on the Vortical and Turbulent Structures in the Lobed jet Flow Using Laser Induced Fluorescence and Particle Image Velocimetry Techniques. *Measurement Science and Technology*, 2000, vol. 11, pp. 698-711

[5] Hu H., Kobayashi T., Saga T., Segawa S., and Tanigushi N., Particle Image Velocimetry and Planar Laser Induced Fluorescence Measurements on Lobed Jet Mixing Flows. *Experiments in Fluids,* 2000, (Suppl.), S141-S157

[6] Hu H., Saga T., Kobayashi T. and Tanigushi N., A Study on a Lobed Jet Mixing Flow by Using Stereoscopic Particle Image Velocimetry Technique. *Physics of Fluids*, 2001, vol. 13(11), pp. 3425-3441

[7] Hu H., Saga T., and Kobayashi T., Dual-Plane Stereoscopic PIV measurements in a lobed jet mixing flow. *AIAA*, 2005, Reno, Nevada 2005-0443

[8] Lockwood F.C., and Moneib A., Fluctuating temperature measurements in a heated round free jet. *Combust Sci Tech*, 1980, vol. 22, pp. 63-81

[9] Mi J., Nobes D., and Nathan G.J., Influence of jet exit conditions on the passive scalar field of an axisymmetric free jet. *J. Fluid Mech*, 2001a, vol. 432, pp. 91-125

[10] Mi J., Nathan G.J., and Nobes D., Mixing characteristics of axisymmetric free jet issuing from a contoured nozzle, an orifince plate and a pipe. *J Fluid Eng*, 2001b, vol.123, pp.878-883

[11] Pitts W.M., Effects of global density ratio on the centerline mixing behavior of axisymmetric turbulent jet. *Exp Fluids*, 1991, vol.11, pp.125-134

[12] Quinn W.R., Effects of nonparallel exit flow on round turbulent free jet. *Int J Heat Fluid Flow,* 1989b, vol. 10, pp.139-145

[13] Quinn W.R., Upstream nozzle shaping effects on near field flow in round turbulent free jets. *Euro J Mech B/Fluids*, 2006, vol.25, pp. 279-301

[14] Nastase I., Meslem A., and Gervais P., Primary and secondary vortical structures contribution in the entrainement of low Reynolds number jet flows. *Experiments in Fluids*, 2008, vol. 44(6), pp.1027-1033

[15] Nastase I., and Meslem A., Vortex dynamics and entrainment mechanisms in low Reynolds orifice jets. *Journal of Visualization*, 2008, vol.11(4), pp.309-318

[16] Zaman K.B.M.Q., Axis switching and spreading of an axisymmetric jet: The role of coherent structure dynamics. *Journal of Fluid Mechanics,* 1996, vol.316, pp.1-27

[17] Ho C.M., and Gutmark E.J., Vortex induction and mass entrainment in a small-aspect ratio elliptic jet. *J. Fluid Mech.,* 1987, vol. 179, pp.383-405

[18] Ho CM, and Gutmark EJ, Vortex induction and mass entrainment in a small-aspect ratio elliptic jet. *J. Fluid Mech.,* 1987, vol. 179, pp. 383

[19] Husain HS, and Hussain AKMF, Controlled excitation of elliptic jets. *Phys. Fluids*, 1983, vol. 26, pp. 2763

[20] Hussain AKMF, and Husain HS, Elliptic jets. Part I. Characteristics of unexcited and excited jets. *J. Fluid Mech.,* 1989, vol. 208, pp. 257

[21] Yoon JH, and Lee SJ, Investigation of the near-field structure of an elliptic jet using stereoscopic particle image velocimetry. *Meas. Sci. Technol,* 2003, vol. 14, pp. 2034-2046

[22] Quinn WR, Streamwise evolution of a square jet cross-section. *AIAA J.,* 1992, vol. 30, pp. 2852

[23] El Hassan M., and Meslem A. Time-resolved stereoscopic PIV investigation on the entrainment in the near field of circular and daisy-shaped orifice jets. *Physics of fluids,* under consideration.

[24] Yule A.J., Lage scale structure in the mixing layer of a round jet. *Journal of Fluid Mechanics*, 1994, vol. 89(413), pp. 413-432

[25] Liepmann D., and Gharib M., The role of streamwise vorticty in the near field entrainement of round jets. *Journal of Fluid Mechanics*, 1992, vol. 245, pp. 642-668

[26] Rogers MM., and Moser RD., The three-dimensional evolution of a plane mixing layer: the Kelvin-Helmholtz rollup. *J. Fluid Mech.,* 1992, vol. 243, pp. 183-226

[27] Foss J.K., Small-scale turbulence in a plane mixing layer. *PhD thesis,* 1994, University of Southern California

[28] Toyoda K., and Hiramoto R., Effect of streamwise vortices on characteristics of jets. *JSME International Journal*, 2006, Series B, vol. 49(4), pp.884-889

[29] McCornick D.C., and Bennett Jr. J.C., Vortical and turbulent structure of a lobed mixer free shear layer. *AIAA journal,* 1994, vol. 32(9), pp. 1852-1859

[30] Mi J., Nathan G.J., and Wong C.Y., PIV measurements of a turbulent jet issuing from round sharp-edge plate. *Exp. Fluids*, 2007, vol.42, pp. 625-637

[31] Prasad A.K., and Adrian R.J., Stereoscopic particle image velocimetry applied to liquid flows. *Exp Fluids*, 1993a, vol. 13, pp. 49-60.

[32] Arroyo M.P., and Greated C.A., Stereoscopic particle image velocimetry. *Meas Sci Technologie*, 1991, vol. 2, pp. 1181-1186

[33] Sinha S.K., and Kuhlman P.S., Investigating the use of stereoscopic particle streak velocimetry for estimating the three-dimensional vorticity field. *Exp Fluids,* 1988, vol. 12, pp. 377-384

[34] Prasad A.K., Stereoscopic particle image velocimetry. *Exp. Fluids*, 2000, vol. 29, pp. 103-116.

[35] Soloff S.M., Adrian R.J., and Liu Z-C, Distorsion compensation for generalized stereoscopic particle image velocimetry. *Meas Sci Technol,* 1997, vol. 8, pp. 1441-1454